EMI R&D PROJECT PROGRESS REPORT

Reporting year	2026
Project Title:	Earth system modeling of PaleOClimatic HyperthermALs (EPOCHAL)
Computer Project Account:	Spitnuri
Principal Investigator(s):	Matteo Nurisso
Affiliation:	CNR-ISAC
Name of ECMWF scientist(s) collaborating to the project (if applicable)	
Start date of the project:	01/01/2025
Expected end date:	31/12/2026

Computer resources allocated/used for the current year and the previous one
(if applicable)
Please answer for all project resources

		Previous year		**Current year**	
		Allocated	Used	Allocated	Used
High Performance Computing Facility	(units)	9,000,000	27,229	14,000,000	2.035.594
Data storage capacity	(Gbytes)	20,000	0	40,000	0

Summary of project objectives

The final objective of the project is to investigate the characteristics of the Early Eocene climate and the mechanism of hyperthermals. To achieve this objective, we are developing a low-resolution and high-efficiency version of the Earth System Model EC-EARTH4, called EC-Earth4 Fast (EC-Earth4-FAST). The model will be tuned separately from the EC-EARTH4 standard resolution model. Orography, bathymetry, and all boundary conditions (BCs) are under adaptation to allow simulations of the required paleoclimate period.

Summary of problems encountered

The main limitation was the delayed release of the EC-Earth4, which prevented simulations with fully interactive vegetation. The LPJ-GUESS dynamic vegetation model became available only with EC-Earth4 version 4.1.4 (November 2025), leaving insufficient time for configuration and testing. The most significant technical challenge was the numerical instabilities encountered in the high-concentration simulations (6× and 9× CO_2). Addressing these issues required substantial effort and a reallocation of project resources to diagnose and mitigate model instabilities under extreme forcing conditions. The current solution, based on a tendency cut-off, should be considered a temporary mitigation measure rather than a definitive fix. Future work will focus on improving the numerical robustness of the convection scheme, with support from ECMWF developers who implement it.

Summary of plans for the continuation of the project

The next phase of the project will focus on completing the refactor of the early Eocene BCs and producing a suite of long-scale (at least 1000 years) DeepMIP-Eocene phase 1 simulations, referred to in the project request as EPOCHAL simulations. These experiments will provide the basis for a comprehensive evaluation of the EC-Earth4-FAST-P configuration under Eocene climate conditions and will support the preparation of the first peer-reviewed publication describing its performance and scientific results.

List of publications/reports from the project with complete references

Coppo, R., Sozza, A., Nurisso, M., Meccia, V., Fabiano, F., and Davini, P.: Unlocking Multi-Millennial Eocene Simulations with a New EC-Earth4 Configuration, EGU General Assembly 2026, Vienna, Austria, 3–8 May 2026, EGU26-10249, https://doi.org/10.5194/egusphere-egu26-10249, 2026.

Summary of results

Low-resolution configuration and CORE simulations

As part of the EPOCHAL project, a new low-resolution configuration of EC-Earth4, termed EC-Earth4-FAST (TL63L31-ORCA2-L31), was developed to enable computationally efficient simulation while retaining the full complexity of a coupled global climate model. The configuration combines OpenIFS cycle 48r4, NEMO 4.2.2, and OASIS5-MCT, with horizontal resolutions of approximately 2.5° in the atmosphere and 2° in the ocean.
Subsequently, the computational performance of this configuration was assessed in detail. Particular attention was devoted to identifying an effective balance between MPI and OpenMP parallelization, especially relevant for OIFS. In addition, the frequency of radiation calculations within OpenIFS was maintained at one call every three model time steps, like in older configurations, which provides a suitable compromise between computational cost and physical accuracy.
Following careful load balancing and performance optimization, the model achieved very promising computational performance, reaching nearly 220 simulated years per day (SYPD) and less than 30 core-hours per simulated year (CHPSY) when running on only 256 cores on ECMWF HPC2020

(Figure 1). This reduces the computational cost by almost a factor of forty compared with the EC-Earth3 CMIP6 configuration. As a result, the model approaches the computational efficiency typically associated with intermediate-complexity climate models, while still retaining the full physical complexity of a full-fledged Global Climate Model. A 2000-year preindustrial control simulation and a 165-year historical simulation were completed to validate the model performance.

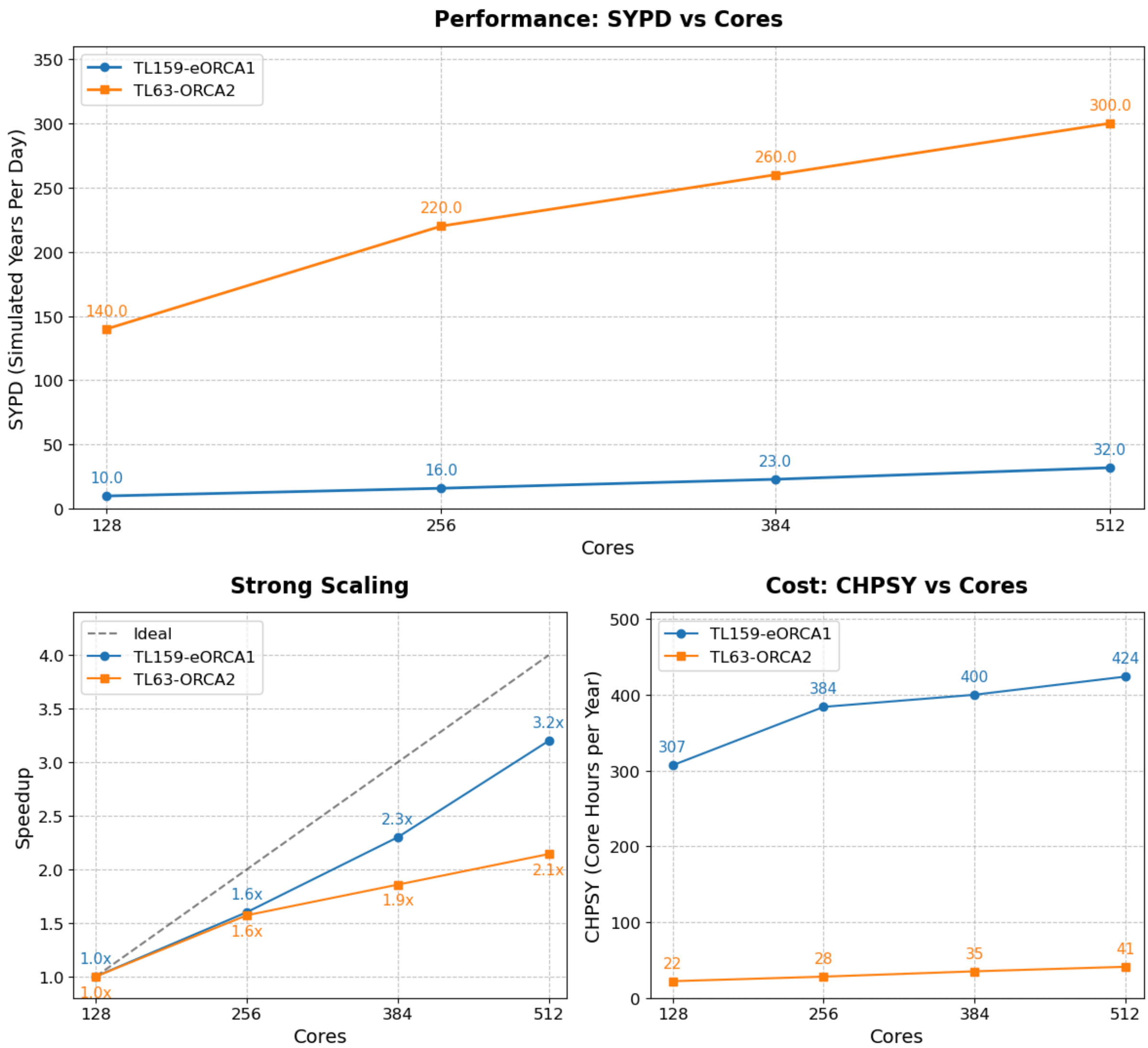

Figure 1 – Performance and scalability analysis of EC-Earth4 configurations on the ECMWF HPC2020 platform. The top panel shows the Simulated Years Per Day (SYPD, i.e., a measure of the speed of the model) for the high-resolution TL159-eORCA1 (blue) and the low-resolution TL63-ORCA2 (orange) configurations. The bottom-left panel displays the Strong Scaling (relative speedup) compared to the ideal linear scaling (dashed line). The bottom-right panel shows the computational cost in Core Hours Per Simulated Year (CHPSY). All metrics are plotted as a function of the number of cores, with baseline performance measured at 128 cores.

As a general overview, we report a scorecard produced with ECmean (Figure 2), an automatic tool for model evaluation developed by CNR-ISAC, for a historical simulation run with the tuned configuration of the TL63-ORCA2.
This reports the values of the Reichler and Kim (2008) performance indices for a set of variables and regions, normalized to the average of a CMIP6 ensemble. The model presents a large bias in sea surface temperature, marked in the southern ocean, which is a well-known bias of EC-Earth3 (Döscher et al., 2021) and EC-Earth4, and probably will require further tuning in the future. However, the overall climatology is comparable to that of CMIP6-class models operating at substantially higher resolution, demonstrating EC-Earth4-FAST’s suitability for long climate integrations.

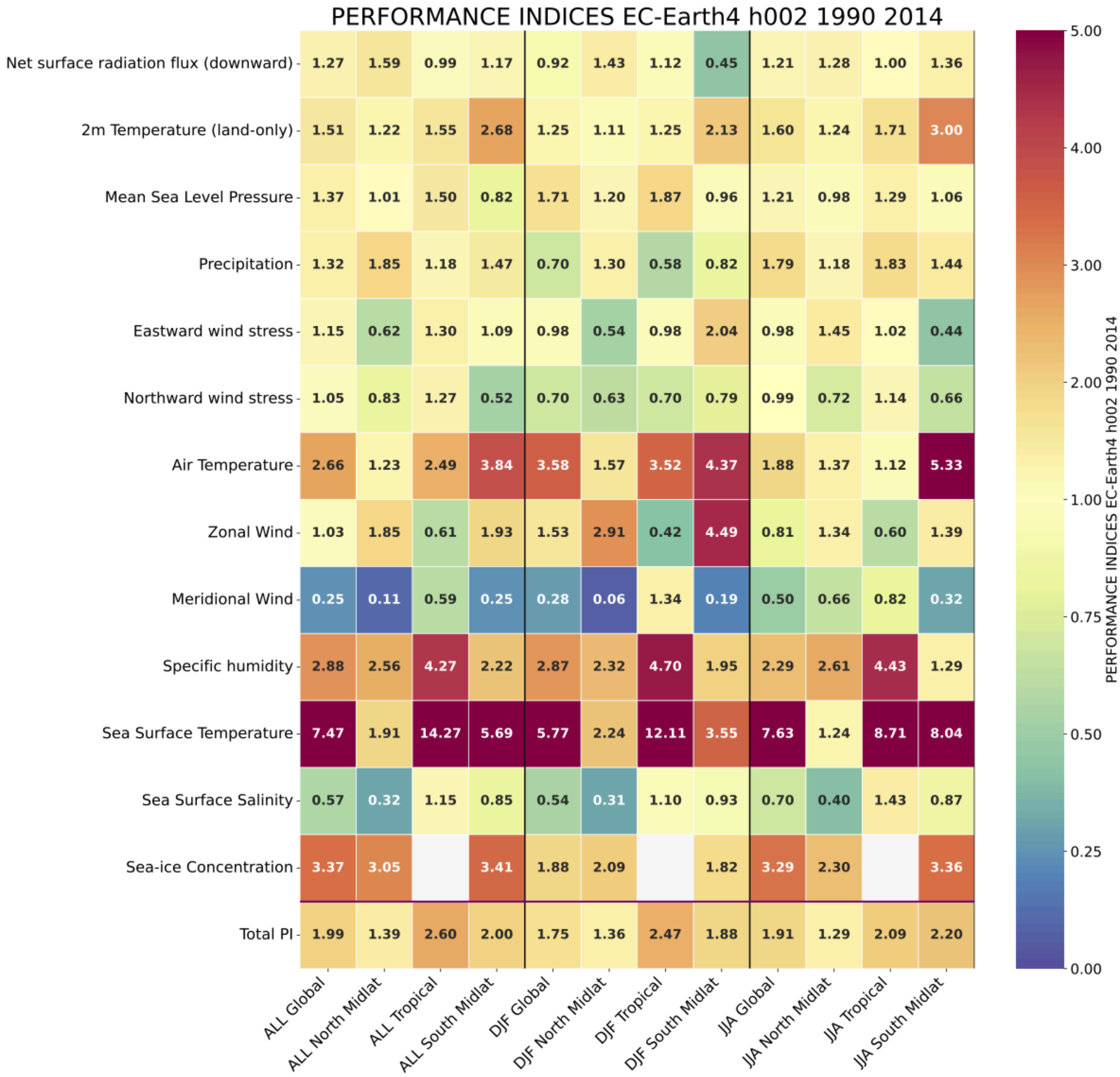

Figure 2 - Reichler and Kim (2008) performance Indices normalized to the CMIP6 average for different regions and seasons for EC-Earth4 TL63-ORCA2 historical simulation from 1990-01-01 to 2014-12-31. Processed regions are Global (90°S-90°N), North Midlat (30°N-90°N), Tropical (30°S-30°N), and South Midlat (90°S-30°S). Numbers < 1 imply better results than the CMIP6 mean.

Eocene Simulations

To enable early Eocene climate simulations, EC-Earth4 required substantial modifications to accommodate deep-time BCs and paleogeographic reconstructions, ranging from implementing a new ocean grid compatible with reconstructed continental positions to defining appropriate atmospheric and oceanic BCs.

The PALEORCA grid

A key development was the integration of the PALEORCA2 ocean grid, originally developed by Institut Pierre-Simon Laplace (IPSL; Sepulcre et al., 2020) for paleoclimate applications. PALEORCA2 provides a more homogeneous grid structure that is better suited to representing ocean circulation under non-modern BCs.

The integration of PALEORCA2 into EC-Earth4 required generating new remapping weights and adapting auxiliary ocean model files to ensure consistency with the new grid geometry. These developments were incorporated into the EC-Earth4 source code and released as part of version 4.1.2. The resulting configuration, termed EC-Earth4-FAST-P (TL63L31-PALEORCA2L31), can be used with both present-day and Eocene paleogeographies and provides the basis for the project's deep-time climate simulations.

Boundary Conditions

To support reproducible paleoclimate experiments, the project developed a complete boundary-condition generation workflow ("Eocene-creator"; https://github.com/renatacoppo/Eocene-creator). The tool generates all EC-Earth4 surface input fields, including land–sea mask, bathymetry, orography, soil parameters, and prescribed vegetation, following the Herold et al. (2014) DeepMIP early Eocene reconstruction (hereafter H14). This infrastructure transforms EC-Earth4-required input files (both boundary and initial conditions) from a present-day climate model into a flexible deep-time modelling platform and constitutes a reusable community resource.

Early Eocene river runoff pathways and drainage basins were reconstructed from paleogrographic flow-direction data and regridded to the model resolution for use in the runoff routing scheme.

Atmosphere and land BCs follow DeepMIP recommendations (Lunt et al., 2017). Preindustrial values were prescribed for the solar constant, orbital parameters, and non-CO2 greenhouse gases. No continental ice sheets are included, and soil properties are set to homogeneous global means derived from the preindustrial simulation. Surface fields such as bare soil albedo and Leaf Area Index (LAI) are prescribed as zonal means from present-day simulations, with specific adjustments over Antarctica.

Orography, subgrid orography parameters, and land-sea mask are taken and adapted from the H14 dataset. Additional parameters, such as lake fraction and the Charnock coefficient, are set to zero.

Vegetation and aerosol distributions were adapted to EC-Earth4 requirements using published translation methodologies (e.g., Zhang et al., 2021).

Oceanic BCs were modified to reflect early Eocene tidal mixing and geothermal heat flux. Paleogeographically consistent tidal dissipations were interpolated onto the PALEORCA2 grid using conservative remapping to preserve global energy, while geothermal heating flux (q) at the ocean floor was prescribed and incorporated into the PALEORCA2 grid using a paleogeographically consistent reconstruction based on the 55 Ma global seafloor age distribution of Müller et al. (2008), and an age-heat-flow relationship from Stein and Sten (1992).

Initial Conditions

Initial conditions were designed to ensure numerical stability and consistency with long centennial-scale integrations. The atmosphere was initialized from a cold start using spectrally truncated fields, retaining only the lowest harmonic to smooth imbalances caused by the changed orography. Specific humidity and snow depth were set to zero to allow the model to develop its own hydrological cycle.

The ocean was initialized with a constant salinity of 34.7 psu following Lunt et al. (2017). Ocean temperature initialization follows the IPSL-based DeepMIP alternative (Zhang et al., 2020), with a vertically uniform deep ocean temperature (10°C below 1000 m) and a zonally symmetric upper-ocean structure, yielding equatorial surface temperatures up to 34°C and polar temperatures of 10°C. Compared to standard DeepMIP initial conditions, this configuration reduces equatorial temperatures by approximately 6°C.

Numerical adjustment

Initial simulations under PETM-like BCs revealed numerical instabilities, primarily linked to the warm climate state pushing atmospheric and oceanic parameterization schemes beyond their

calibrated range. A first mitigation step consisted of reducing the atmospheric and oceanic time steps (3600 s to 2700 s, and 5400 s to 2700 s, respectively), resulting in an overall effective model throughput of approximately 30%, and a production rate of about 160 SYPD.
Further instabilities occurred in high-CO2 experiments (especially on 6xCO2 and 9xCO2 configurations), where the convection scheme occasionally produced unphysical updrafts under extreme near-surface cooling. These were addressed by introducing a damping limiter that constrains convection tendencies beyond a predefined threshold, enabling stable multi-century integration under warm-climate conditions while remaining largely inactive under present-day forcing. With this modification in place, EC-Earth4 can run stably for several hundred simulated years under 6×CO_2 configurations.
Using EC-Earth v4.1.4 on ECMWF HPC2020, fully coupled DeepMIP-style equilibrium simulations were performed for 1×, 3×, and 6× CO_2 concentrations, each integrated for 200 years, achieving exceptional computational performance slightly below 200 SYPD.
The resulting simulations were evaluated against the DeepMIP intercomparisons to assess large-scale temperature patterns and polar amplification under high-CO2 climates.

Temperature response

The global mean near-surface air temperature response of the EPOCHAL simulations is shown in Figure 3 as a function of atmospheric CO_2 concentration and compared with the DeepMIP ensemble (Lunt et al., 2021). While DeepMIP models exhibit broadly consistent equilibrium climate sensitivity (ECS) (~4.5 ºC per CO2 doubling), EC-Eart4 simulations show systematically higher global mean temperatures across all forcing levels, exceeding the ensemble mean by approximately 4–5 °C. The resulting ECS is ~6.6ºC per CO2 doubling, about 2ºC higher than the DeepMIP average.

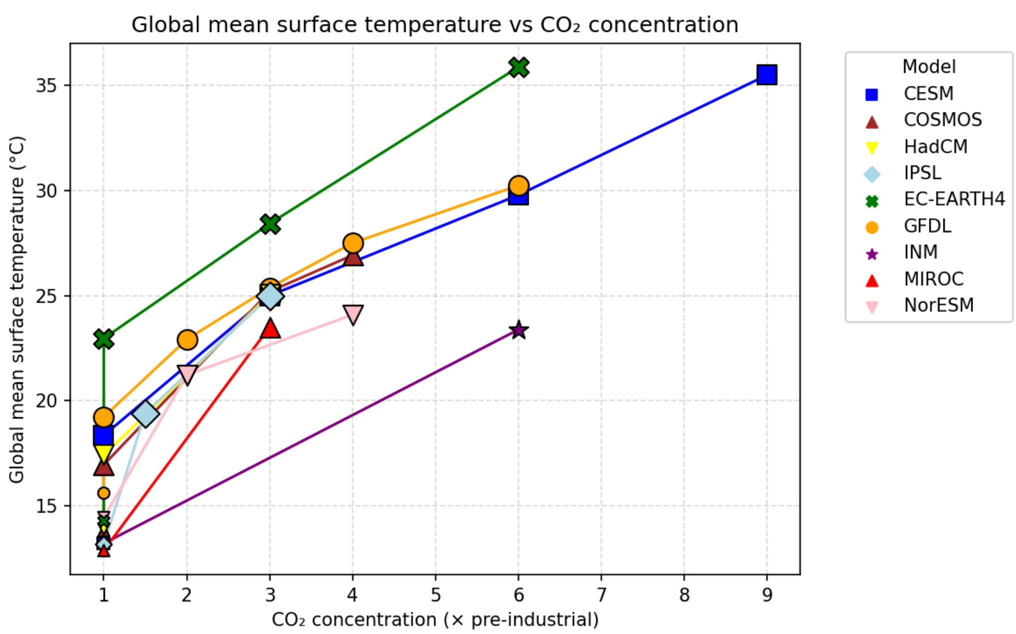

Figure 3 - Global annual mean near-surface (2 m) air temperature in the EC-Earth (green crosses) and DeepMIP ensemble, as a function of atmospheric CO2. Large coloured symbols show the Eocene simulations, and smaller coloured symbols show the associated preindustrial controls. The models that have carried out Eocene simulations at more than one CO2 concentration are joined by a straight line. (derived from Lunt et al., 2021).

Despite this offset, the simulated meridional sea surface temperature (SST) gradient (shown in Figure 4 as the average SST equatorwards of ±30° minus the average SST polewards of ±60°, as a function of global mean SST) follows the same general tendency as the DeepMIP ensemble, decreasing with warming and closely resembling CESM-like responses, although EC-Earth4 consistently exhibits higher global mean SSTs for each CO_2 concentration.

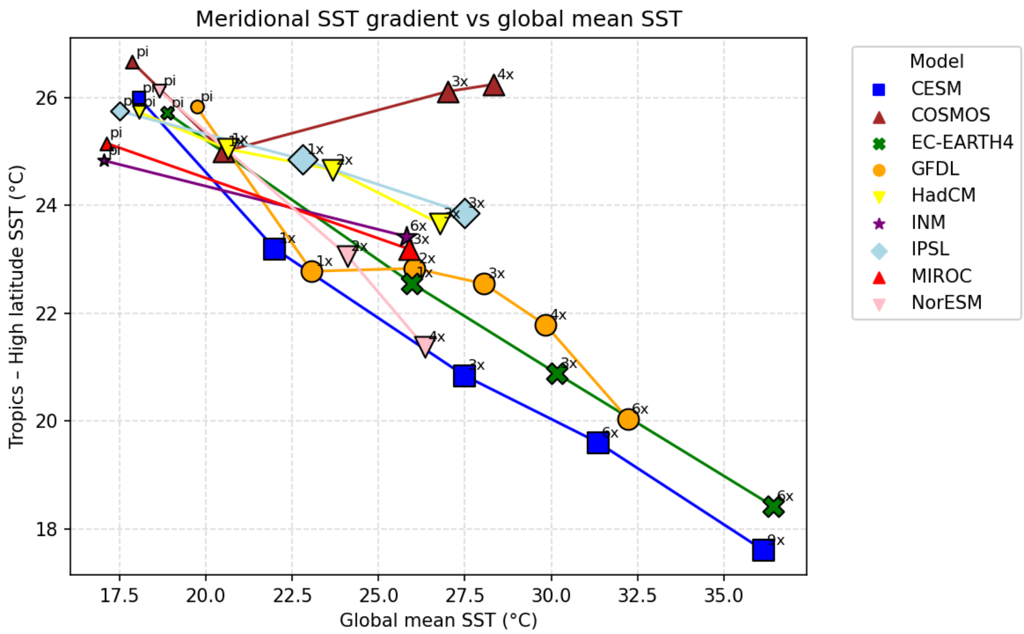

Figure 4 - Meridional SST gradient as a function of global mean SST in the EC-Earth (green crosses) and DeepMIP simulations. The meridional SST gradient is defined here as the average SST equatorwards of ±30°minus the average SST polewards of ±60°. Large coloured symbols show the Eocene simulations, and smaller coloured symbols show the associated preindustrial controls. The models that have carried out Eocene simulations at more than one CO2 concentration are joined by a straight line. (Adapted from Lunt et al., 2021)

Polar amplification is robust across all experiments (Figure 5), with amplification factors of ~2.2, 1.91, and 1.69 for the $1\times CO_2$, $3\times CO_2$, and $6\times CO_2$ experiments, respectively, and is consistently stronger in the Southern Hemisphere due to the absence of Antarctic ice sheets and associated changes in albedo and elevation. The $1\times CO_2$ case already shows strong amplification, highlighting the dominant role of paleogeographic BCs in setting the baseline climate state.

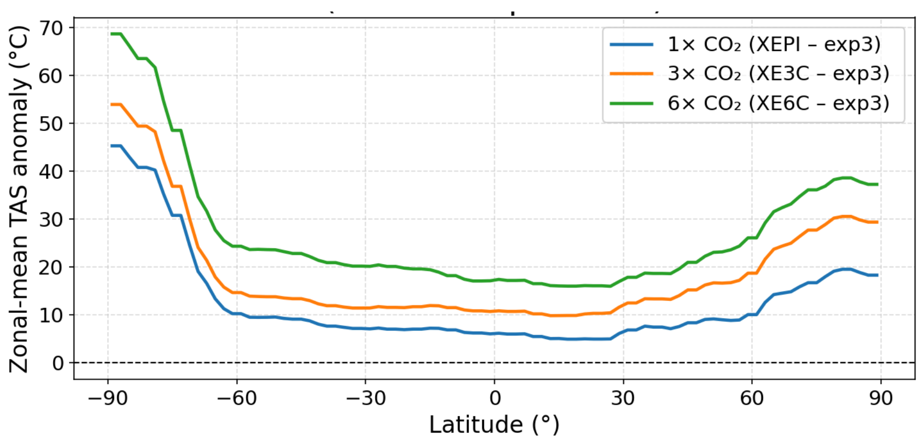

Figure 5 - Zonal mean near-surface air temperature in the Eocene simulations, as a function of latitude and prescribed atmospheric CO2 concentration, expressed as anomalies relative to the equivalent preindustrial control.

Spatial temperature anomalies (Figure 6) are broadly consistent with CESM, GFDL, and HadCM3 patterns, including enhanced warming at high latitudes, over land relative to ocean, and over regions affected by reduced orography (e.g., Tibetan Plateau). Ocean warming (Figure 7) is strongest in high-latitude basins, particularly the Southern Ocean and North Atlantic, with weaker tropical anomalies and a reduced equator-to-pole gradient.

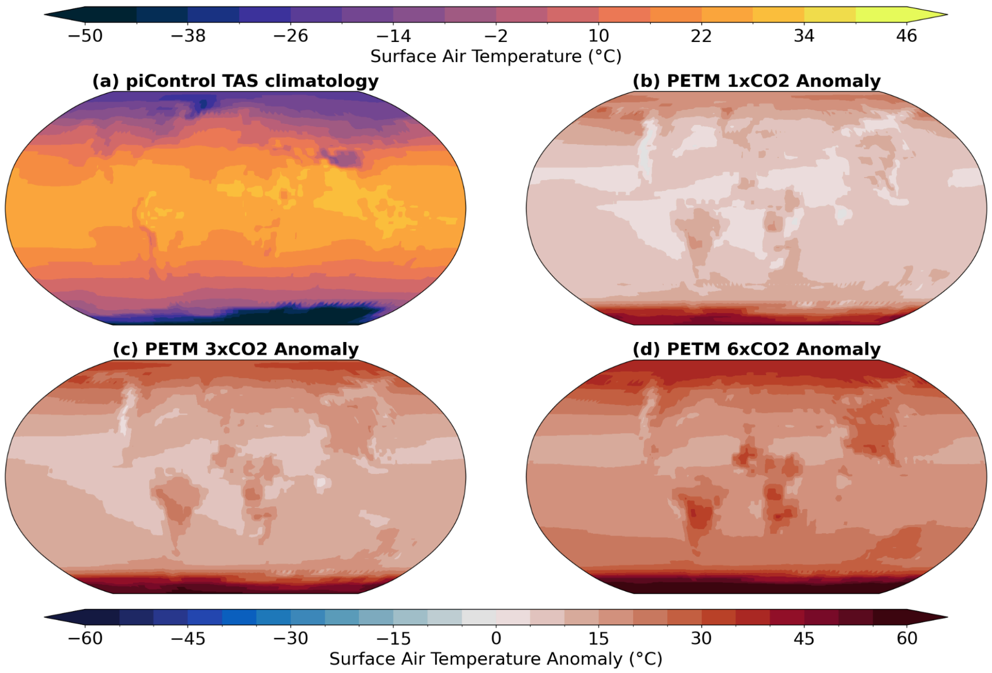

Figure 6 - Mean annual near-surface air temperature for the piControl simulation (a), and temperature anomalies for the Eocene simulations relative to the piControl zonal mean (b–d), ordered by increasing CO_2 concentration.

Across higher CO2 simulations, the temperature spatial patterns persist with increasing amplitudes. Persistent North Pacific warming may indicate changes in ocean circulation and deep-water formation, suggesting enhanced poleward heat transport, although a detailed dynamical analysis is left for future work.

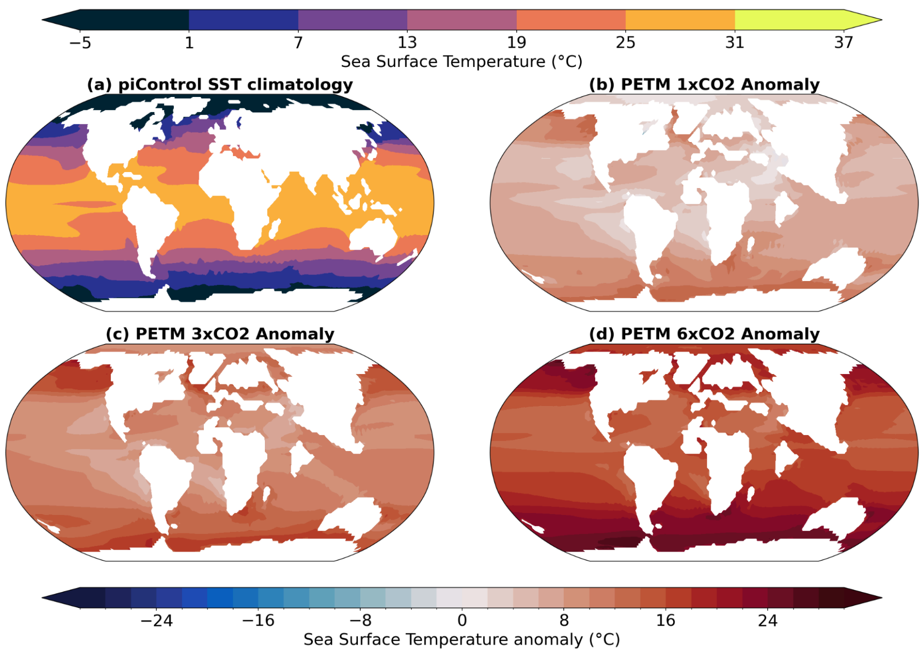

Figure 7 - Mean annual sea surface temperature for the piControl simulation (a), and sea surface temperature anomalies for the Eocene simulations relative to the piControl zonal mean (b–d), ordered by increasing CO_2 concentration.

References

Döscher, R., Acosta, M., Alessandri, A., Anthoni, P., Arneth, A., Arsouze, T., ... & Zhang, Q. (2021). The EC-earth3 Earth system model for the climate model intercomparison project 6. Geoscientific Model Development Discussions, 2021, 1-90. https://doi.org/10.5194/gmd-15-2973-2022

Herold, N., Buzan, J., Seton, M., Goldner, A., Green, J. A. M., Müller, R. D., ... & Huber, M. (2014). A suite of early Eocene (~ 55 Ma) climate model boundary conditions. Geoscientific Model Development, 7(5), 2077-2090. https://doi.org/10.5194/gmd-7-2077-2014

Lunt, D. J., Huber, M., Anagnostou, E., Baatsen, M. L., Caballero, R., DeConto, R., ... & Zeebe, R. E. (2017). The DeepMIP contribution to PMIP4: Experimental design for model simulations of the EECO, PETM, and pre-PETM (version 1.0). Geoscientific Model Development, 10(2), 889-901. https://doi.org/10.5194/gmd-10-889-2017

Lunt, D. J., Bragg, F., Chan, W. L., Hutchinson, D. K., Ladant, J. B., Morozova, P., ... & Otto-Bliesner, B. L. (2021). DeepMIP: Model intercomparison of early Eocene climatic optimum (EECO) large-scale climate features and comparison with proxy data. Climate of the Past, 17(1), 203-227. https://doi.org/10.5194/cp-17-203-2021

Müller, R. D., Sdrolias, M., Gaina, C., & Roest, W. R. (2008). Age, spreading rates, and spreading asymmetry of the world's ocean crust. Geochemistry, Geophysics, Geosystems, 9(4). https://doi.org/10.1029/2007GC001743

Reichler, T., & Kim, J. (2008). Uncertainties in the climate mean state of global observations, reanalyses, and the GFDL climate model. Journal of Geophysical Research: Atmospheres, 113(D5). https://doi.org/10.1029/2007JD009278

Sepulchre, P., Caubel, A., Ladant, J. B., Bopp, L., Boucher, O., Braconnot, P., ... & Tardif, D. (2019). IPSL-CM5A2. An Earth System Model designed for multi-millennial climate simulations. Geoscientific Model Development Discussions, 2019, 1-57. https://doi.org/10.5194/gmd-13-3011-2020

Stein, C. A., & Stein, S. (1992). A model for the global variation in oceanic depth and heat flow with lithospheric age. Nature, 359(6391), 123-129. https://doi.org/10.1038/359123a0

Zhang, Q., Berntell, E., Axelsson, J., Chen, J., Han, Z., De Nooijer, W., ... & Yang, S. (2021). Simulating the mid-Holocene, last interglacial and mid-Pliocene climate with EC-Earth3-LR. Geoscientific Model Development, 14(2), 1147-1169. https://doi.org/10.5194/gmd-14-1147-2021

Zhang, Y., Huck, T., Lique, C., Donnadieu, Y., Ladant, J. B., Rabineau, M., & Aslanian, D. (2020). Early Eocene vigorous ocean overturning and its contribution to a warm Southern Ocean. Climate of the Past, 16(4), 1263-1283. https://doi.org/10.5194/cp-16-1263-2020